Asociación Argentina de Astronomía
BAAA, Vol. 47, 2004
P. Cincotta, G. Dubner, S. Malaroda, C.H. Mandrini, H. Muriel, G.E. Romero y R. Vázquez, eds.
INFORME INVITADO – INVITED REVIEW

On the origin of magnetic fields in Astrophysics

Daniel O. Gómez
Instituto de Astronomía y Física del Espacio,
Casilla de Correo 67, Sucursal 28, (1428) Buenos Aires, Argentina,
gomez@iafe.uba.ar

Abstract. Magnetic fields play an important role in a wide variety of astrophysical objects, such as planets, stars, accretion disks, galaxies and galactic clusters. The magnetic fields associated to these objects display large differences in their origin, morphologies and intensities, which therefore makes their theoretical modelling much more difficult. The most promising mechanism to explain the origin of astrophysical magnetic fields is the so-called dynamo effect, which consists of an efficient transfer of kinetic energy of astrophysical plasma flows into magnetic energy. The use of supercomputers to model high Reynolds numbers plasma flows, allowed in recent years to test the ability of certain flows to generate magnetic fields. In the present study, we review our current knowledge on the origin of the magnetic fields in several astrophysical objects.
Resumen. Los campos magnéticos desempeñan un rol importante en una amplia gama de objetos astrofísicos, tales como planetas, estrellas, discos de acreción, galaxias y cúmulos de galaxias. Los campos magnéticos asociados a estos objetos, presentan fuertes diferencias en cuanto a su orígen, morfología e intensidad, lo cual representa un desafío para su explicación teórica. El mecanismo más promisorio de generación de campo magnético es el llamado efecto dínamo, que consiste en la transformación de energía cinética en magnética. En los últimos años, la disponibilidad de supercomputadoras ha permitido investigar cuantitativamente la capacidad de diversos flujos astrofísicos (caracterizados por su elevado número de Reynolds) para generar campos magnéticos. En este trabajo se reseñará nuestro conocimiento actual sobre el orígen de los campos magnéticos en distintos objetos astrofísicos.

1. Introduction

The aim of the present paper is to provide an updated overview of our current observational and theoretical knowledge of the role played by magnetic fields in astrophysics. This is a rather ambitious task, since magnetic fields pervade virtually all known astrophysical objects, including planets, stars, accretion disks, galaxies and clusters of galaxies, and therefore the present review is necessarily far from complete.
We focus on the theoretical mechanisms proposed in the literature for the origin of magnetic fields in different astrophysical environments, and whenever available, on their associated observational signatures. In section 2 we briefly describe the fluidistic description known as magnetohydrodynamics, which is the general theoretical framework to be used. A summary of the so-called α-Ω dynamos is

given in section 3, and an overview on turbulent dynamos is shown in section 4. The observed properties of the solar magnetic field, as well as the theoretical models applied, are listed in section 5, and a bird's eye overview of our current knowledge of stellar magnetic fields is given in section 6. Galactic magnetic fields are discussed in section 7, and the overall conclusions of the present study are summarized in section 8.

2. The magnetohydrodynamic description

Magnetohydrodynamics (MHD) corresponds to a fluidistic description of matter and its interaction with magnetic fields, which appropriately describes the large-scale dynamics of fully ionized plasmas. By large scales, we mean typical sizes much larger than the mean free path of the particles and timescales much longer than the inverse of the collisional frequency.

2.1. The MHD equations

Incompressible MHD is described by the induction and the Navier-Stokes equations,

$$\frac{\partial \boldsymbol{B}}{\partial t} = \nabla \times (\boldsymbol{U} \times \boldsymbol{B}) + \eta \nabla^2 \boldsymbol{B} \tag{1}$$

$$\frac{\partial \boldsymbol{U}}{\partial t} = -(\boldsymbol{U} \cdot \nabla)\,\boldsymbol{U} + (\boldsymbol{B} \cdot \nabla)\,\boldsymbol{B} - \nabla\left(P + \frac{B^2}{2}\right) + \boldsymbol{F} + \nu \nabla^2 \boldsymbol{U}\ , \tag{2}$$

with the divergence-free conditions $\nabla \cdot \boldsymbol{U} = \nabla \cdot \boldsymbol{B} = 0$ for the velocity and magnetic fields. The external force $\boldsymbol{F}$ is assumed to be solenoidal, and the velocity $\boldsymbol{U}$ and magnetic field $\boldsymbol{B}$ are expressed in units of a characteristic speed U_0. The scalar field P is the fluid pressure divided by the constant mass density, while η and ν are the magnetic diffusivity and the kinematic viscosity. The vector potential $\boldsymbol{A}$ is defined by $\boldsymbol{B} = \nabla \times \boldsymbol{A}$.

2.2. Extra effects: Hall, electron pressure and ambipolar diffusion

One-fluid MHD, as presented in equations (1)-(2), is the standard framework used to describe the large-scale dynamics of astrophysical plasmas. For instance, it is a good approximation for the solar dynamo and the geodynamo (Priest & Forbes 2000).

However, astrophysical scenarios characterized by low temperatures, partial ionization, or collisionless plasmas, are not properly described by the MHD framework, since MHD fails to distinguish the relative motions between different species. A first step toward creating a more appropriate theory for these scenarios is to include the dominant two-fluid effects considered in the generalized Ohm's law. The most relevant effects for astrophysical applications are ambipolar diffusion and the Hall effect (Zweibel 1988, Wardle 1999, Balbus & Terquem 2001, Sano & Stone 2002).

Ambipolar diffusion is important in the evolution of magnetic fields in protostars and proto-planetary circumstellar disks, as well as in the dynamics of the galactic gas (Zweibel 1988, 2002; Sano & Stone 2002, Brandenburg & Subramanian

2004). It is also relevant in the evolution of magnetic clouds (Zeldovich et al. 1983). In the interstellar medium, ambipolar diffusion is believed to be the principal mechanism responsible for breaking the frozen-in condition for the magnetic field.

The ambipolar drift occurs because the magnetic field lines are attached to the plasma ions but not to the neutrals. The Lorentz force acting over the magnetized ions generates a drift between the ions and the neutrals. If collisions are frequent, the Lorentz force acting on the ions is balanced by collisions with the neutrals. Under these assumptions, in a partially ionized medium with the bulk velocity $\boldsymbol{U}$ dominated by the neutrals, the induction equation (1) takes the form

$$\frac{\partial \boldsymbol{B}}{\partial t} = \nabla \times [(\boldsymbol{U} + \lambda \boldsymbol{J} \times \boldsymbol{B}) \times \boldsymbol{B}] + \eta \nabla^2 \boldsymbol{B} \, , \tag{3}$$

where $\lambda = (\rho_i \upsilon_{in})^{-1}$. Here, ρ_i is the ion mass density, and υ_{in} is the collision frequency between ions and neutrals. Note that in this approximation $\boldsymbol{U}_i = \boldsymbol{U} + \lambda \boldsymbol{J} \times \boldsymbol{B}$ is the velocity of the ions, and equation (3) expresses that the magnetic field lines in the ideal case (i.e. $\eta = 0$) are frozen to the ion velocity field.

The Hall effect is relevant in dense molecular clouds (Wardle & Ng 1999), in accretion disks (Wardle 1999, Balbus & Terquem 2001, Sano & Stone 2002) in white dwarfs and neutron stars (Yakovlev & Urpin 1980, Muslimov 1994, Geppert & Rheinhardt 2002), and in the early universe (Tajima et al. 1992). Recently, the impact of the Hall current on the dynamo effect was also measured in the laboratory (Ding et al. 2004).

With the inclusion of the Hall effect, the induction equation (1) reads

$$\frac{\partial \boldsymbol{B}}{\partial t} = \nabla \times [(\boldsymbol{U} - \varepsilon \boldsymbol{J}) \times \boldsymbol{B}] + \eta \nabla^2 \boldsymbol{B} \, , \tag{4}$$

The Hall term $\varepsilon \boldsymbol{J} \times \boldsymbol{B}$ is the manifestation of the difference in velocity between ions and electrons. Indeed, in a two-species quasi-neutral electron-ion plasma $\boldsymbol{U}_e = \boldsymbol{U} - \varepsilon \boldsymbol{J}$ is the electron velocity. From equation (4), when $\eta = 0$ the magnetic field is frozen to the electron velocity field, instead of the bulk velocity $\boldsymbol{U}$ as is the case in one-fluid MHD.

Assuming the characteristic velocity equal to the Alfvén velocity, the intensity of the Hall effect is given by $\varepsilon = c/(\omega_{pi} L_0)$, where c is the speed of light and ω_{pi} is the ion plasma frequency. Note that c/ω_{pi} is the ion skin depth, which is the lenghtscale where the Hall effect becomes non-negligible. Typical values of ε for several astrophysical objects can be found in Mininni et al. (2003).

Since in equation (4) the magnetic field is stretched by the electron velocity field $\boldsymbol{U}_e$ rather than the bulk velocity field $\boldsymbol{U}$, and these velocities can be quite different, the Hall term is expected to impact on dynamo mechanisms.

3. Alpha-Omega dynamos

According to the so-called $\alpha - \Omega$ theoretical models, the dynamo is caused by a combination of differential rotation (the Ω effect) and the role of the turbulent small-scale fluid motions (the α effect).

A dynamo is a mechanism able to generate a macroscopic magnetic field from an initial micro-scale configuration, consisting of a small seed magnetic field along with a substantial velocity field. The first theoretical model of such a mechanism, was developed within the general framework of *mean-field theory* by Krause & Radler (1980). More recently, Blackman & Field (1999) presented the so-called *reduced smoothing approximation* (RSA), which is summarized below. We assume the initial state $\boldsymbol{u}_0$, $\boldsymbol{b}_0$ to be a solution of equations (1)-(2) in the absence of a large-scale field. We now perturb the system about this micro-scale solution, with $\boldsymbol{B} = \overline{\boldsymbol{B}} + \boldsymbol{b} + \boldsymbol{b}_0$ and $\boldsymbol{U} = \overline{\boldsymbol{U}} + \boldsymbol{u} + \boldsymbol{u}_0$, where the overbar denotes spatially or statistically averaged large-scale fields, while $\boldsymbol{u}$ and $\boldsymbol{b}$ are small-scale perturbations. Note that while $\boldsymbol{b}_0$ is the short-scale magnetic field in the absence of $\overline{\boldsymbol{B}}$, $\boldsymbol{b}$ is the perturbation when $\overline{\boldsymbol{B}}$ is present, which might not be isotropic. All small-scale fields have zero averages, while their products in general do not. Substituting into equations (1)-(2), using the equation for $\boldsymbol{b}_0$ and taking averages, we find an equation for the evolution of the large-scale averaged magnetic field,

$$\frac{\partial \overline{\boldsymbol{B}}}{\partial t} = \nabla \times \left(\overline{\boldsymbol{U}} \times \overline{\boldsymbol{B}} \right) + \langle \nabla \times \left(\boldsymbol{u}_0 \times \boldsymbol{b} + \boldsymbol{u} \times \boldsymbol{b}_0 \right) \rangle \ , \tag{5}$$

where quadratic terms in $\boldsymbol{b}$ and $\boldsymbol{u}$ were dropped, as is usually done in mean field theory. Note that, although a common assumption, it is not clear that these terms will remain negligible once the mean field grows to finite amplitudes. Therefore, the RSA assumption is less restrictive than the one used in mean field derivations.

We can also derive an equation for the small-scale perturbed magnetic field $\boldsymbol{b}$. Here, we drop terms involving spatial derivatives of the mean fields because the variations of the long-scale fields are negligible on the microscale. Finding corrections to the α coefficient as our current focus, we also ignore the averaged terms as they will not contribute to the equation for $\overline{\boldsymbol{B}}$. We obtain

$$\frac{\partial \boldsymbol{b}}{\partial t} = \nabla \times \left(\boldsymbol{u}_0 \times \overline{\boldsymbol{B}} - \boldsymbol{b}_0 \times \overline{\boldsymbol{U}} \right) \ . \tag{6}$$

In a similar manner, we can write the perturbed Euler equation,

$$\frac{\partial \boldsymbol{u}}{\partial t} = \left(\nabla \times \boldsymbol{b}_0 \right) \times \overline{\boldsymbol{B}} - \left(\overline{\boldsymbol{U}} \cdot \nabla \right) \boldsymbol{u}_0 - \nabla p \ , \tag{7}$$

From the divergence of Eq. (7), we obtain $p = -\boldsymbol{b}_0 \cdot \overline{\boldsymbol{B}}$ for the small-scale pressure perturbation, which, when substituted in Eq. (7), yields

$$\frac{\partial \boldsymbol{u}}{\partial t} = \left(\overline{\boldsymbol{B}} \cdot \nabla \right) \boldsymbol{b}_0 - \left(\overline{\boldsymbol{U}} \cdot \nabla \right) \boldsymbol{u}_0 \tag{8}$$

To obtain an expression for α, we close equation (5) by approximating the time derivatives in (6) and (8) by multiplications by an inverse correlation time. Assuming a weakly anisotropic turbulence and eliminating terms involving $\overline{\boldsymbol{U}}$ in the short-scale equations in the proper reference frame, the evolution equation for the mean field $\overline{\boldsymbol{B}}$ becomes

$$\frac{\partial \overline{\boldsymbol{B}}}{\partial t} = \nabla \times \left(\overline{\boldsymbol{U}} \times \overline{\boldsymbol{B}} + \alpha \overline{\boldsymbol{B}} \right) \ , \tag{9}$$

where $\alpha\overline{\boldsymbol{B}}$ denotes the microscale contribution to the magnetic field generation with

$$\alpha = \tau(- < \boldsymbol{u}_0 \cdot \nabla \times \boldsymbol{u}_0 > + < \boldsymbol{b}_0 \cdot \nabla \times \boldsymbol{b}_0 >)/3 \ . \tag{10}$$

The kinetic term is proportional to the kinetic helicity of the flow, i.e. $H_k = \frac{1}{2}\int \boldsymbol{U} \cdot \boldsymbol{\omega}\, dV$ (Krause & Radler 1980). According to the present derivation, the expresion of α is modified by a magnetic correction derived by Pouquet et al. (1976). Equation (9) describes the large-scale dynamics of the magnetic field, for a given large-scale velocity profile $\overline{\boldsymbol{U}}$ usually describing differential rotation (the Ω effect), and considering the effect of a small-scale MHD turbulence through the α coefficient (the α effect). $\alpha - \Omega$ models have been extensively used to describe the generation of magnetic fields in a variety of rotating objects, such as the Sun, stars, accretion disks or galaxies.

4. Turbulent dynamos

In the so-called turbulent dynamos, the small-scale turbulence that was theoretically modeled through the α coefficient, is described in a more detailed fashion by direct numerical simulations (DNS). The simulations discussed in this section were made using a parallel pseudospectral code (Mininni et al. 2003, 2004; Gómez et al. 2005). Equations (1)-(2) are integrated in a cubic box with periodic boundary conditions. The code uses a second order Runge-Kutta scheme to evolve the equations in time, and the 2/3-rule to control aliasing error (Canuto et al. 1988). As a result, the largest wavenumber k_{max} that can be resolved in a spatial grid of N^3 points is given by $k_{max} = N/3$.

We performed several simulations with 256^3 spatial grid points and $\eta = \nu = 0.02$. Simulations begin by subjecting the Navier-Stokes equation to a stationary helical force $\boldsymbol{F}$ operating at a macroscopic scale $k_{force} = 3$ (Mininni et al. 2003) to reach a hydrodynamic turbulent steady state. The resulting statistically steady state is characterized by a positive kinetic helicity. As discussed in the previous section, the kinetic helicity is known to play a significant role in generating magnetic fields through the so-called α-effect.

Once the hydrodynamic stage of the simulation reaches a steady state, a non-helical and very weak magnetic seed was introduced. This initial magnetic seed was generated by a δ-correlated vector potential centered at $k_{seed} = 35$. The run was continued with the same external helical force in the Navier-Stokes equation, to study the growth of magnetic energy due to dynamo action.

Figure 1(a) shows the spatial distribution of one of the components of the magnetic field right after the seed has been implanted, for a purely MHD run with 256^3 grid points. Figure 1(b) shows the shift toward much larger spatial scales by about the time when the dynamo reaches saturation. Both the exponentially fast growth of magnetic energy and its net flow toward larger spatial scales, are the essential ingredients for a turbulent dynamo. Within this context, turbulent dynamos can be defined as those turbulent microscale flows with the ability to generate large-scale magnetic fields.

Figure 2 shows the kinetic and magnetic spectra at different times. The dotted curve at the lower right, corresponds to the spectrum of the magnetic seed. During the initial kinematic stage, the magnetic energy grows uniformly at all wave numbers. After the saturation ($t \approx 5$) the emergence of a large-scale field

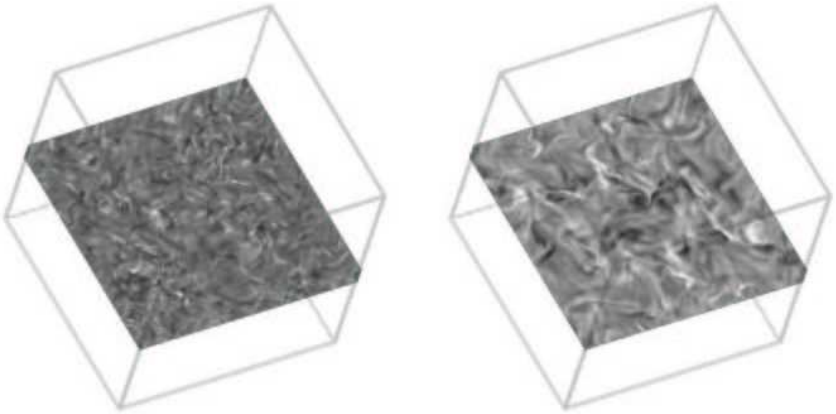

Figura 1. Slice of a 256^3 MHD simulation displaying the component of magnetic field perpendicular to the slice. Left: right after inserting the magnetic seed. Right: when the stationary regime is reached.

can be clearly seen in the spectrum. At $t \approx 18.4$, when the system has already reached equipartition, the magnetic energy at large scales (small wave numbers) still remains growing slowly. As a result, the large scale magnetic field reaches super-equipartition with the kinetic energy. An excess of magnetic energy can be also observed at small scales.

The slope of the total (magnetic plus kinetic) energy spectrum in the inertial range is consistent with Kolmogorov's law (i.e. $E_k = \varepsilon^{2/3} k^{-5/3}$) and in good agreement with simulations of helical MHD turbulence with higher spatial resolution (Haugen et al. 2003).

The effect of ambipolar diffusion in the dynamo was studied using a simplified model by (Zweibel 1988), and an α-effect was recovered from equation (3). It was shown that helical turbulence can amplify a magnetic field under these conditions, and ambipolar diffusion can alleviate the need of large turbulent diffusivity in some numerical models of galactic dynamos. More recently Brandenburg & Subramanian (2000) confirmed the existence of an α-effect contributed by ambipolar diffusion, using both direct simulations in a periodic box and a closure model. Simulations with the modified version of the induction equation given in Eqn. 3 have also been made within the context of reconnection in the interstellar medium (Zweibel & Brandenburg 1997). The generation of sharp fronts together with a change in the reconnection rate of magnetic fields was observed in this study.

Using mean field theory, Mininni et al. (2002) showed that a helical flow can amplify a magnetic field in the Hall-MHD framework, and obtained a generalized expression for the α-effect. The Hall term was found to enhance or suppress dynamo action depending on the value of ε. DNS of Hall-MHD helical dynamo action confirmed this result (Mininni et al. 2003, 2004).

The saturation amplitude of the Hall-MHD dynamo has a nonlinear dependence with the amplitude of the Hall effect ε. When the Hall lengthscale is close to or smaller than the Kolmogorov's magnetic dissipation scale $k_\eta = (\langle J^2 \rangle / \eta^2)^{1/4}$, the MHD behavior is recovered ($\varepsilon \ll 1$) and no differences in the evolution and

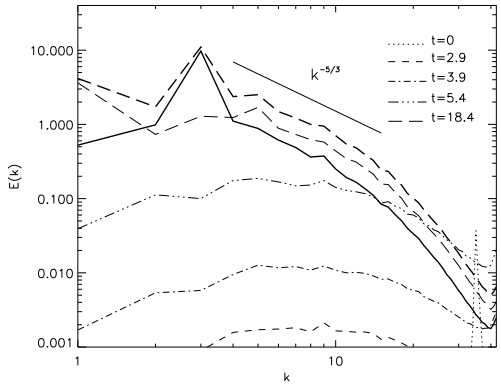

Figura 2. Mean kinetic energy spectrum (thick line), total energy spectrum (thick dashed line), and magnetic energy spectrum at different times ($\epsilon = 0$ and $R = 300$). The Kolmogorov's slope is shown as a reference.

saturation of the dynamo can be identified. On the other hand, when the Hall effect dominates in all the relevant scales including the energy containing scales of the turbulent flow ($\varepsilon \approx 1$), the helical dynamo is less efficient than its MHD counterpart. The dynamo saturates at a lower level of total magnetic energy, and the kinetic energy dominates the dynamics at almost all scales.
However, there is an intermediate regime in which the dynamo effect is enhanced by the Hall term. In this regime, the Hall effect dominates the dynamics in a range of scales starting from intermediate scales and up to the diffusion scale. The enhancement was observed to increase as the Reynolds numbers and the scale separation are increased (Mininni et al. 2004), and the peak of maximum magnetic energy moves to smaller values of ε as R is increased. Also, in this regime the Hall effect was observed to alleviate the slow saturation of the MHD helical dynamo, and large scale magnetic fields grow faster than its MHD counterpart.

5. Solar magnetic field

The solar magnetic field is believed to be regenerated every 11 years by a dynamo process operating at the *"tachocline"*, which is a thin layer located at the base of the convective region. According to the $\alpha - \Omega$ theoretical models, the solar dynamo is caused by a combination of the differential rotation in this layer (the Ω-effect) and the role of the turbulent small-scale fluid motions (the α-effect). Once the field emerges at the surface, it creates bipolar regions in the corona, whose footpoints correspond to sunspots at photospheric heights. Sunspot locations are not completely random: they tend to concentrate along two bands at both sides of the equator, as shown in Fig. 3. At the beginning of the cycle, the first sunspots appear near a belt at latitudes of approximately 30°. The region of activity widens up and slowly migrates toward the equator as the cycle evolves. According to dynamo theory, the number of sunspots and their spatial

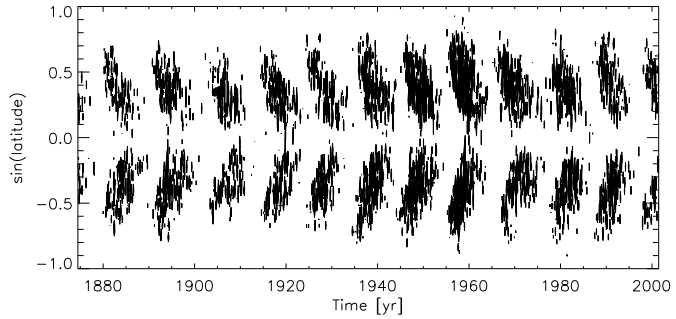

Figura 3. Butterfly diagram from Royal Greenwich Observatory.

distribution is in phase with the strong toroidal magnetic field at the base of the convective region (Stix 1976). The observational discoveries of Hale's law (Hale 1908) and the reversal of the polar magnetic field (Babcock 1961), led to the conclusion that the sunspot cycle is a manifestation of a roughly periodic evolution of the Sun's magnetic field, with a mean period of 22 years.
The kinematic dynamo approximation, corresponds to the assumption of a given velocity field $\boldsymbol{U}(\boldsymbol{r},t)$ in which the magnetic field $\boldsymbol{B}(\boldsymbol{r},t)$ is advected according to

$$\frac{\partial \boldsymbol{B}}{\partial t} = \nabla\times(\boldsymbol{U}\times\boldsymbol{B}) + \nabla\times(\alpha\boldsymbol{B}) + \eta\nabla^2\boldsymbol{B}\ , \tag{11}$$

In spherical coordinates and assuming axisymmetry, the magnetic field can be decomposed into its toroidal and poloidal components, i.e. $\boldsymbol{B} = B_\phi\hat{\phi}+\nabla\times(A\hat{\phi})$. The flow is given by $\boldsymbol{U} = r\sin\theta\,\Omega(r,\theta)\hat{\phi}+\nabla\times(\Psi(r,\theta)\hat{\phi})$, where Ω describes the differential rotation of the Sun, and $\Psi(r,\theta)$ determines a slow meridional flow (θ is the colatitude). The functions $\Omega(r,\theta)$ and $\Psi(r,\theta)$ were derived from recent helioseismic observations (see for instance Mininni & Gómez 2004). Typical values for the angular velocity are $\Omega \approx 2\ 10^{-6}$ rad s^{-1} (the solar core rotates like a rigid body at approximately this speed), and the meridional flows are about 20 m s^{-1}. The coefficient α in Eqn (11) represents the effect of small scale convective motions on the large scale magnetic field $\boldsymbol{B}(\boldsymbol{r},t)$. The effect of α is essential for the regeneration of the poloidal field, while its role in the evolution of the toroidal component is negligible for the Sun. The generally assumed expresion for α is

$$\alpha = \alpha(\boldsymbol{B}) = \frac{\alpha_0}{1+(\frac{B}{B_{sat}})^2}\sin(\theta)\cos(\theta)\ . \tag{12}$$

It contains a nonlinearity responsible for the saturation of magnetic energy growth, which simulates the inhibition of turbulence caused by the Lorentz force on the fluid. According to observations, this saturation value can be estimated as $B_{sat} \approx 10^5$ G. The value chosen for alpha is $\alpha_0 \approx 15$ cm s^{-1}, to yield results compatible with observations (Choudhuri 1992, Hoyng 1993).
Since the dynamo activity on the Sun is concentrated in the *"tachocline"* (Charbonneau & Dikpati 2000), we can simply replace the radial derivatives by the

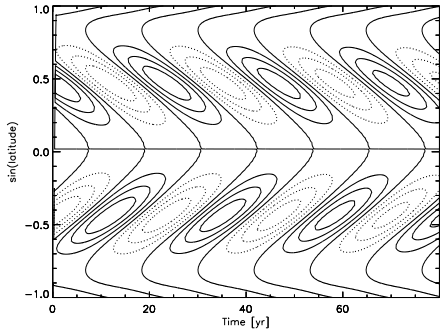

Figura 4. Contours of toroidal magnetic field. The maximum magnetic field is 10^5 G. Full traces correspond to positive levels and dotted traces to negative levels.

inverse width of this layer (approximately $0.1R_\odot$). A numerical integration of Eqn. 11 under this simplifying assumption, provides the spatio-temporal evolution of the toroidal (i.e. $B_\phi(\phi,t)$) and poloidal ($A(\phi,t)$) magnetic field components.
Figure 4 shows the toroidal magnetic field intensity as a function of latitude and time. These results reproduce many of the regularities observed in the solar cycle, such as its time periodicity, the equatorward migration of the regions of magnetic activity, the change of magnetic polarity from one cycle to the next and from one hemisphere to the other.

6. Stellar magnetic fields

The Sun is not the only star displaying the signatures of a cyclic dynamo. Late-type stars, which have outer convective regions just like the Sun, also present magnetic fields. The magnetic strength increases with the rotation speed of the star. Rapid rotators such as the T Tauri stars, have average magnetic intensities of a few kilogauss. Main sequence stars of spectral types between G0 and K7 also show cyclic variations in their magnetic stengths, as measured by the ratio of Calcium H and K emission lines (Baliunas et al. 1995).
There are three important dimensionless parameters to study the cyclic magnetic activity in late-type stars: *(1)* the Rossby number, which is the ratio between the rotation period of the star and the turnover time of eddies in its convective region (i.e. $Ro \approx T_{rot}/T_{conv}$); *(2)* the ratio of magnetic cycle to rotation period, i.e. T_{cyc}/T_{rot}; *(3)* the ratio of chromospheric Calcium H and K emissivities to the bolometric flux, R_{HK}. The observational study of many cyclic stars led to the following empirical relationships for these parameters (Saar & Brandenburg 2001)

$$\frac{T_{cyc}}{T_{rot}} \propto Ro^{\sigma} \propto R_{HK}^{-\sigma'} \tag{13}$$

Scatter plots show the presence of two groups of stars: *active stars* for which $\sigma_A \approx 0.46$ and $\sigma'_A \approx 0.85$, and *inactive stars* for which $\sigma_I \approx 0.48$ and $\sigma'_I \approx 0.72$.

Although α-Ω theoretical models have been developed to reproduce these empirical laws (see an overview in Brandenburg & Subramanian 2005), they require speculative hypothesis about the α-quenching mechanism, in order to obtain a quantitative agreement.
Early-type stars also present magnetic fields. Peculiar Ap and Bp stars show magnetic fields of typically $1 - 10$ kG, even though they are slow rotators. Furthermore, these stars have inner convective cores, which poses a strong limitation to dynamo models (Moss 2001). On the other hand, their magnetic and rotational periods coincide for most of the stars observed. Therefore, a reasonable theoretical model seems to be a *displaced dipole* model, rotating along with the star. Even though many important questions remain unanswered, this simple model provides a good first approximation for the observed magnetic variations in most of the Ap and Bp stars.

7. Galactic and extra-galactic magnetic fields

At larger scales, the interstellar gas in galaxies and the intergalactic gas in clusters of galaxies is also permeated by magnetic fields. The mechanisms involved in generating these magnetic fields are still uncertain, but there are essentially two competing theories: *(1) the primordial theory*, according to which the magnetic field was generated in the initial stages of the Universe, and is currently being advected by the dynamics of the galaxies; *(2) dynamo theory*, in which the field is generated by an α-Ω mechanism by the galaxes themselves (Zweibel & Heiles 1997, also Brandenburg & Subramanian 2005).
Although observations might in principle distinguish between these two theoretical viewpoints, there is at present no conclusive evidence to rule out any of them, and therefore more observations and theoretical analysis are clearly necessary. Observations of other galaxies allow a global view of their magnetic fields, which is supplemented by spatially more detailed observations of the magnetic field of the Milky Way. Observations consists mainly on the intensity, polarization and Faraday rotation of the diffuse synchrotron radiation. In the case of our galaxy, we also have measurements of the Zeeman splitting to determine the line-of-sight component, as well as detailed polarization maps to derive the orientation of the field in the plane of the sky.
There are at least two clear examples of spiral galaxies, showing magnetic field-lines aligned with the spiral arms: NGC6946 (Beck & Hoermes 1996) and NGC5055 (Beck 1996). By looking at the symmetries of magnetic fields in spiral galaxies, we can classify them in two groups: *(1) axisymmetric spirals (ASS)* are those presenting even parity with respect to a rotation of 180° about the galactic center (see Fig. 5a), and *(2) bisymmetric spirals (BSS)* are those displaying an odd parity (see Fig. 5b). Dynamo theory is in principle consistent with ASS configurations (and a quadrupolar transverse structure, see Fig. 5c), while on the other hand primordial theories would lead to BSS configurations and a dipolar structure accross the disk (see Fig. 5d). Our galaxy, for instance, displays field reversals in the radial direction, thus suggesting the possibility of a BSS configuration (Zweibel & Heiles 1997). There are a couple of galaxies whose global magnetic field structure is consistent with ASS (M31 and IC342), while M81 is better described by a BSS configuration (Brandenburg & Subramanian

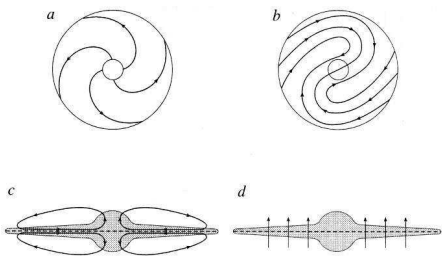

Figura 5. Cartoons of magnetic field configurations (adapted from Zweibel & Heiles 1997) for: (a) face-on view of ASS, (b) face-on view of BSS, (c) edge-on view of even-parity magnetic structure, (d) edge-on view of odd-parity magnetic structure

2005). Most galaxies, however, do not seem to be described by any of these symmetries, but by a superposition of modes.

8. Conclusions

The sustained improvement in spatial resolution and innovative observational techniques in virtually all spectral ranges, permitted a considerable progress in our current understanding about the origin and the role played by magnetic fields in a variety of astrophysical environmenT.
On the other hand, parallel numerical codes allow to simulate different configurations of astrophysical plasmas, which are characterized by very large Reynolds numbers. Because of this, a sustantial progress in turbulent dynamos has been made in recent years.
It seems clear that the role played by magnetic fields are essential in many astrophysical systems, modifying the dynamics of the gas and in turn being distorted and re-generated by this dynamical state. Notwithstanding, this self-consistent state is still far from being understood, which calls for more high-quality observations and innovative theoretical models in the near future.

Acknowledgments. I would like to acknowledge to the Scientific Committee of the 47th Annual Meeting of the *Asociación Argentina de Astronomía* for their invitation, and to the Local Organizing Committee for their kind hospitality. I am also grateful to an anonymous referee for his/her constructive comments.

References

Babcock, H.W. 1961, ApJ, 133, 572.

Balbus, S. A., & Terquem, C. 2001, ApJ, 552, 235

Baliunas, S. L., Donahue, R. A., & Soon, W. H. 1995, ApJ, 438, 269.

Beck, R., & Hoernes, P. 1996, Nature, 379, 47-49.

Beck, R. 1996, Astron. Soc. Pacific, C.S. 97, 475.

Blackman, E.G. & Field, G.B. 1999, ApJ, 521, 597

Brandenburg, A. & Subramanian, K. 2000, A&A, 361, L33

Brandenburg, A., & Subramanian, K. 2005, arXiv:astro-ph/0405052.

Canuto, C., Hussaini, M. Y., Quarteroni, A., & Zang, T. A. 1988, "Spectral Methods in Fluid Dynamics". Springer-Verlag, New York

Charbonneau, P., & Dikpati, M. 2000, ApJ, 543, 1027.

Choudhuri, A.R. 1992, A&A, 253, 277.

Ding, W. X. et al. 2004, Phys.Rev.Lett, 93, 045002.

Geppert, U. & Rheinhardt, M. 2002, A&A, 392, 1015

Gómez, D. O., Mininni, P. D., and Dmitruk, P. 2005, Phys. Scripta, in press.

Hale, G.E. 1908, ApJ, 28, 315.

Haugen, N. E. L., Brandenburg, A., and Dobler, W. 2003, ApJ, 597, 141

Hoyng, P. 1993, A&A, 272, 321.

Krause, F. & Radler, K.H. 1980, "Mean-field MHD and dynamo theory", Pergamon Press.

Mininni, P., & Gómez, D. 2002, ApJ, 573, 454.

Mininni, P. D., Gómez, D. O., & Mahajan, S. M. 2002, ApJ, 567, L81

Mininni, P. D., Gómez, D. O., & Mahajan, S. M. 2003, ApJ, 587, 472

Mininni, P. D., & Gómez, D. O. 2004, A&A, 426, 1065.

Mininni, P. D., Gómez, D. O., & Mahajan, S. M. 2005, ApJ, 619, 1019.

Moss, D. 2001, Amer. Soc. Pacific C.S., 248, 305.

Muslimov, A. G. 1994, MNRAS, 267, 523

Pouquet, A., Frisch, U., & Léorat, J. 1976, J. Fluid Mech., 77, 321

Priest, E., & Forbes, T. 2000, "Magnetic reconnection", Cambridge Univ. Press.

Saar, S., & Brandenburg, A. 2001, Amer. Soc. Pacific C.S., 248, 231.

Sano, T., & Stone, J. M. 2002, ApJ, 570, 314

Stix, M. 1976, A&A, 47, 243.

Tajima, T., Cable, S., Shibata, K., & Kulsrud, R. M. 1992, ApJ, 390, 309

Wardle, M. 1999, MNRAS, 307, 849

Wardle, M., & Ng, C. 1999, MNRAS, 303, 239

Yakovlev, D. G. & Urpin, V. A. 1980, Astr. Zh., 57, 526

Zeldovich, Ya.B., Ruzmaikin, A.A., & Sokoloff, D.D. 1983, "Magnetic fields in astrophysics, Gordon & Breach, New York.

Zweibel, E. G. 1988, ApJ, 329, 384

Zweibel, E. G. & Brandenburg, A. 1997, ApJ, 478, 563

Zweibel, E.G., & Heiles, C. 1997, Nature, 385, 131.